

2715

# Effect of Spiral Reinforcement in Composite Columns

M. Tsuji, H. Okamura, and R. Harashima

*Reprinted from*

Transactions of the Japan Concrete Institute 1979

【V-2】

## EFFECT OF SPIRAL REINFORCEMENT IN COMPOSITE COLUMNS

Masanori Tsuji\*, Hajime Okamura\* and Ryuichi Harashima\*\*

## ABSTRACT

This paper describes the effect of spiral reinforcement in composite columns consisting of steel pipe and mortar evaluating by the proposed analytical method which was derived from the test results of 45 specimens. This analytical method can be applied to the composite column subjected not only to axial loading but also to bending moment until the maximum loading capacity is reached. The effect of spiral reinforcement can be considered to increase mortar strength only after the strain of mortar or the deflection of the member becomes extremely large. Therefore, the effect of spiral reinforcement reduces rapidly as the slenderness ratio of member increases.

## INTRODUCTION

Composite columns consisting of steel pipe and mortar are being used in construction of Seikan Under Sea Tunnel, and they are reinforced with spirals where the earth pressure is particularly large. This method is employed from the economical view point by Japan Railway Construction Public Corporation after confirming the remarkable effects of spiral reinforcement against axial loading (1)(2). However, experiments have not been conducted for the case of being subjected to bending moment in addition to axial loading, although the effects of spirals in this case is questionable. This study was conducted to clarify the effects of spiral reinforcement in such cases.

## OUTLINE OF THE TESTS

A total of 45 specimens were made, of which 37 were subjected to central compression and 8 to eccentric compression. Specimens were all of cylindrical shape with height of three times of the diameter. The outline of the tests is summarized in Table 1. In case of the eccentric compression tests, the amounts of eccentricity were selected to be 10 percent of the diameter of the specimens, which resulted in 7.5 mm smaller due to the friction of the loading equipments.

---

\* Department of Civil Engineering, University of Tokyo

\*\* Japan Railway Construction Public Corporation

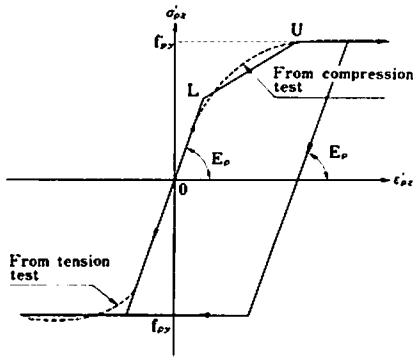


Fig. 1 Stress ( $\sigma_{pz}$ )-strain ( $\epsilon_{pz}$ ) relation of the steel pipe

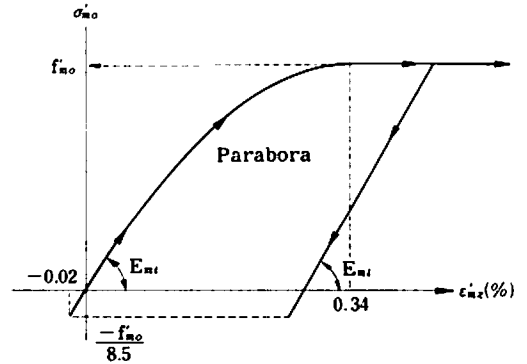


Fig. 2 Stress ( $\sigma'_{mo}$ )-strain ( $\epsilon'_{mz}$ ) relation of the mortar ( $E_{mi}$ : Initial tangent modulus)

Table 1 Outline of the test program

Diameter of spiral bars, mm	9	13			16	22	No spiral
Pitch of the spiral, mm	20	20	30	40	30	32	
Diameter of pipe, mm	140	7*(3)*	2				2
	165	2	4*	4*	2	9*(3)*	4
	247						5*(1)
	318						4*(1)

Numbers indicate the total number of specimens.

( ) indicates the number of specimens using deformed bars.

\* indicates that specimens subjected to eccentric compressive test are included.

Table 2 Properties of steel pipes

Diameter (mm)	Thickness (mm)	L*		U*	
		stress (MPa)	strain (%)	stress (MPa)	strain (%)
140	4.5	313	0.16	395	1.44
165	4.5	293	0.14	375	1.30
267	9.3	318	0.20	404	1.96
319	10.3	221	0.12	364	2.00

\* See Fig. 1.

Table 3 Properties of spiral reinforcement

Diameter (mm)	Designation*	Yield stress (MPa)	Ultimate strength (MPa)
9	R	301	432
13	R	305	456
	D	387	592
16	R	283	418
	D	388	591
22	R	298	459
	D	344	529

\* R:Round bar; D:Deformed bar

## NUMERICAL ANALYSIS

### (1) Stress and Strain in a Section

The stresses between the steel pipe and the encased mortar can be ignored (3)(4). Then, the axial load and bending moment acting on a section can be obtained from integration of the axial stress, and the product of the stress and the distance between the point and the center of gravity, respectively.

The axial stress of a steel pipe can be calculated, when the strain is given by using the stress-strain relationship which has been determined from the compression test of pipes of a complete section and the tension test of the specimen taken from the pipe. An example of the relationship is shown in Fig. 1 together with a simplified relation used in this analysis. The values of the point L and U in the figure are given in Table 2. The yield stress and tensile strength of bars used for spiral reinforcement are given in Table 3.

The axial stress of the mortar encased by the spiral reinforcement can not be easily obtained. For the evaluation of the effect of spirals, it seems important to express the behaviour of mortar under triaxial stresses as a simple formula. In this analysis the axial compressive stress of mortar ( $\sigma_{mz}'$ ) is assumed to be equal to the sum of that in the case of without spirals ( $\sigma_{mo}'$ ) and that proportional to the normalized compressive stress ( $\sigma_{m\theta}'$ ) caused by the spirals.

$$\sigma_{mz}' = \sigma_{mo}' + K\sigma_{m\theta}' \quad \dots (1)$$

The stress  $\sigma_{mo}'$  is obtained from the simplified stress-strain relationship expressed with a parabola and a straight line as shown in Fig. 2. The compressive strengths  $f_{mo}'$ , which were obtained from the standard cylinder tests, were between 31 MPa and 53 MPa, and most of which were more than 45 MPa. The compressive strain at the maximum stress is assumed to be 0.34%, and the stress beyond this strain is assumed to be constant, considering the effect of steel pipe. The Poisson's ratio ( $\nu_{mo}$ ) of mortar within the compressive strain of 0.34% was measured and simplified for analysis as shown in Fig. 3.

The coefficient K in equation 1 is taken as a function of axial strain as shown in Fig. 4. Where the axial compressive strain ( $\epsilon_{mz}'$ ) is smaller than 0.2%, the mortar is regarded as an elastic material, and it is taken to be constant where the axial compressive strain is larger than 0.76%. The value of this coefficient is determined by referring the results of the central compression tests of this study.

It is generally accepted that the stress  $\sigma_{m\theta}'$  is a function of the tensile stress of spiral reinforcement ( $\sigma_{r\theta}$ ).

$$\sigma_{m\theta}' = k_r \sigma_{r\theta}, \quad k_r = A_r / (r_r s_r) \quad \dots (2)$$

where,  $A_r$ ,  $r_r$  and  $s_r$  is the area, radius and pitch of the spiral, respectively.

As the spiral reinforcement is considered to be elastic before yielding, the stress  $\sigma_{r\theta}$  is expressed as follows.

$$\sigma_{r\theta} = E_r \epsilon_{r\theta} - \nu_r \sigma'_{rz} + k \nu_r \sigma_{m\theta} \quad \dots (3)$$

$$\sigma_{m\theta} = -\sigma'_{m\theta}, \quad k = s_r / (2\phi_r), \quad \phi_r : \text{diameter of bar}$$

The axial stress acting to the spiral ( $\sigma_{rz}$ ) should be between zero and the stress calculated by applying the Bernoulli-Euler's assumption to the spiral. Therefore, calculation were made by using these extreme cases.

$$\left. \begin{aligned} \sigma'_{rz} &= 0 && \text{or} \\ \sigma'_{rz} &= E_r \epsilon'_{rz} - \nu_r \sigma_{r\theta} - k \nu_r \sigma_{m\theta} \end{aligned} \right\} \quad \dots (4)$$

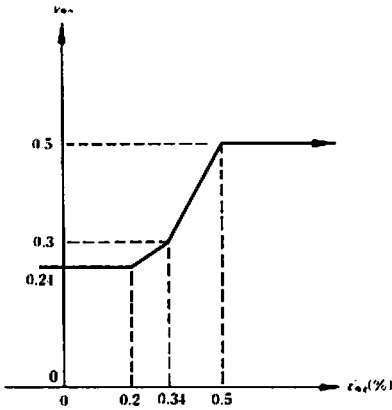


Fig. 3 Poisson's ratio of mortar ( $\nu_{m0}$ )

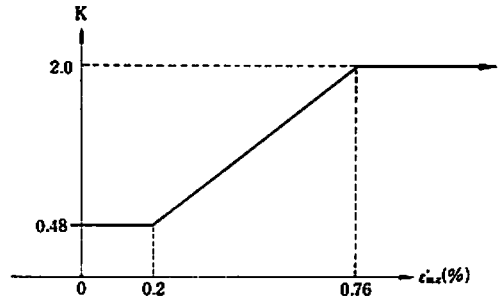


Fig. 4 Coefficient K in equation 1

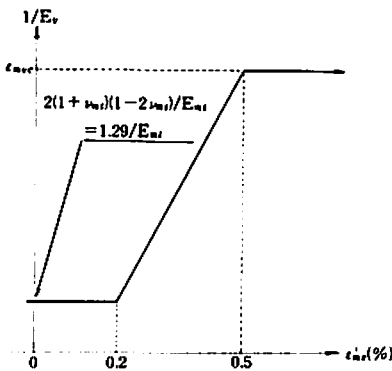


Fig. 5 Coefficient ( $1/E_v$ ) in equation 5

The strain  $\epsilon_{r\theta}$  in equation 3 can be expressed by the strain  $\epsilon_{m\theta}$ , since the integration of the spiral strain  $\epsilon_{r\theta}$  around the spiral is equal to that of the mortar strain  $\epsilon_{m\theta}$ .

The strain  $\epsilon_{m\theta}$  is determined from the volumetric behaviour of mortar under triaxial stresses. In this analysis the volumetric strain of mortar ( $\epsilon_{mv}$ ) is assumed to be the sum of that in case of without spirals ( $\epsilon_{mvo}$ ) and that proportional to the stress  $\epsilon_{m\theta}$ .

$$\epsilon_{mv} = \epsilon_{mvo} + (1/E_v)\sigma_{m\theta} \quad \dots (5)$$

The coefficient  $(1/E_v)$  is taken as the function of the axial compressive strain ( $\epsilon'_{mz}$ ) as shown in Fig. 5. As the strain of the spiral direction ( $\epsilon_{m\theta}$ ) is assumed equal to that of the radial direction ( $\epsilon_{mr}$ ), the volumetric strains are expressed as follows.

$$\epsilon_{mv} = \epsilon_{mz} + 2\epsilon_{m\theta} \quad \dots (6)$$

$$\epsilon_{mvo} = (1-2\nu_{mo})\epsilon_{mz} \quad \dots (7)$$

$$\epsilon_{mz} = -\epsilon'_{mz}$$

From equations 5, 6 and 7, the following equation is obtained.

$$\epsilon_{m\theta} = (0.5/E_v)\sigma_{m\theta} - \nu_{mo}\epsilon_{mz} \quad \dots (8)$$

However, the mortar is assumed to be cracked where the axial tensile strain of mortar ( $\epsilon_{mz}$ ) is larger than 0.02%, and the strain  $\epsilon_{m\theta}$  is derived from the assumption that the axial stress ( $\sigma_{mz}$ ) is zero.

$$\epsilon_{m\theta} = (1-\nu_{mi})\sigma_{m\theta}/E_{mi} \quad : \quad \epsilon_{mz} > 0.02\% \quad \dots (9)$$

$$\nu_{mi} = 0.24 \text{ (see Fig. 3)}$$

Thus, the relation between the axial compressive stress of mortar ( $\epsilon'_{mz}$ ) and the axial load applied was derived.

## (2) Lateral Displacement of a Member

The relation between load and displacement of a member is derived by integration of the curvature of section calculated according to (1). Although the secondary moment due to the lateral displacement is generally small enough to be ignored in ordinary reinforced concrete, it becomes considerably large in the composite member with spiral reinforcement even in the case of the specimen whose height is only three time of the diameter. Therefore, calculations were made considering the secondary moment. In the first step, the displacement at the center of the member is given. Then, the axial load is computed by assuming the curvature at the section. According to the finite difference method, the displacement along the member is computed by step by step. Unless the displacement at the end of member is within the allowable limit, the calculation is repeated by adjusting the curvature at the center. The calculations are continued by increasing the displacement at the center until the load reaches the maximum.

## EVALUATION OF THE ANALYTICAL METHOD

Table 4 shows the summary of the comparison of the test results and calculated values. The comparisons are made at four stages: axial compress-

sive strain ( $\epsilon_{mz}^1$ ) of 0.3, 1 and 3%, and the ultimate load. The strain  $\epsilon_{mz}^1$  of 1% is in the range where the spirals come effective. The mean values of the ratios of calculated load to measured one under the central compressive loading at the strain of 1% and 3% are between 0.98 and 0.99, respectively, with the standard deviations of 0.03 and 0.08. These values are similar to those at the strain of 0.3% where the effect of spirals is negligibly small. In this table two calculated values based on the extreme assumptions regarding to the axial stress of the spiral ( $\sigma_{rz}$ ) are shown. These results clarify that the effect of spiral reinforcement can be traced by either method of this analysis. Spacing of spiral reinforcement used in the tests were between 20 mm and 40 mm or between 10% and 25% of the diameter of spiral. Within this range the spacing of spiral reinforcement does not seem to affect the behaviour of columns with the same amount of reinforcement. No difference in the behaviour of deformed bars and round bars for spiral reinforcement were observed.

An example of stress-strain relation under the eccentric compressive loading is shown in Fig. 6. It is clearly shown in figure and in Table 4 that this analysis can trace the behaviour of the composite columns under the eccentric compressive loading by using the coefficient  $E_v$  which was obtained from the central compressive tests.

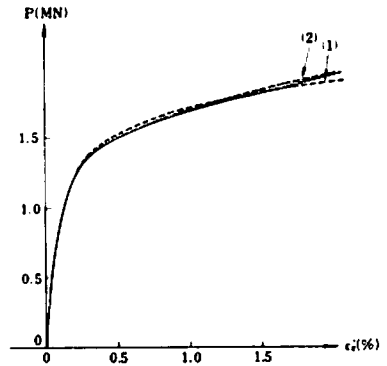


Fig. 6 An example of load (p)-compressive fiber strain ( $\epsilon_1^c$ ) relationship

Table 4 Summary of comparison of calculated and measured values

Test	Strain (%) or Deflection (mm)	Average (1)		Standard deviation (1)	
		(i)	(ii)	(i)	(ii)
Central loading	0.3 %	1.05	1.03	0.08	0.08
	1.0 %	0.98	0.98	0.08	0.07
	3.0 %	0.99	0.99	0.04	0.03
	U (2)	1.02	1.02	0.08	0.08
Eccentric loading	0.3 % (3)	0.99	0.97	0.09	0.09
	1.0 % (3)	1.02	1.02	0.08	0.08
	2.0 % (3)	1.00	1.02	0.07	0.07
	U (2)	0.96	0.99	0.06	0.06
	0.5 mm (4)	1.01	1.01	0.09	0.10
	1.0 mm (4)	0.99	1.00	0.10	0.11
	1.5 mm (4)	0.96	0.98	0.10	0.10
	2.0 mm (4)	0.94	0.97	0.08	0.08

(1) Ratio of the calculated load to the measured one.

(i) Calculated by assuming the  $\sigma_{rz}$  to be zero.

(ii) Calculated by assuming the Bernoulli-Euler's assumption.

(2) Ultimate strength

(3) Extreme fiber strain at compressive side

(4) Difference of deflection between at the middle and at the quarter height

## EFFECT OF SPIRAL REINFORCEMENT

Spiral reinforcement can improve the strength and ductility of mortar under the large deformation by confining the mortar as to be under triaxial compressive stresses. The effect of spiral reinforcement on the ultimate strength of section can be considered as the effect of increasing the strength of mortar, so that the spiral reinforcement is effective to sustain the axial load. However, it is not so effective to sustain the bending moment. Fig. 7 shows the comparison of the effectiveness of the spiral reinforcement and increasing the thickness of the steel pipe having equal stress-strain relationship and equal strength. The effectiveness of spiral reinforcement on load carrying capacity of cross section might be similar to that of increasing the thickness of steel pipe when the eccentricity of load is less than approximately 20 percent of the eccentricity at balanced failure. However, it might be reduced as the eccentricity increase and it becomes less than 50 percent of the effectiveness of steel pipe when the eccentricity is larger than at balanced failure.

As spiral reinforcement comes to be effective only after the deflection of member becomes extremely large, the effectiveness of spiral reinforcement on load carrying capacity of the member is considerably reduced. Fig. 8 shows that the effectiveness of spiral reinforcement on the load carrying capacity of member is similar to that of steel pipe when the slenderness ratio is less than 10. However, it is reduced due to the secondary moment as the slenderness ratio becomes larger.

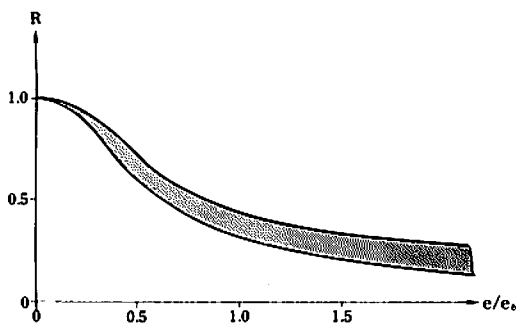


Fig. 7 Effect of spiral reinforcement on load carrying capacity of cross section (R:Ratio of the increase in load carrying capacity of cross section by spiral reinforcement to that by increasing the thickness of steel pipe with equal yield strength, e:Eccentricity of load,  $e_b$ :Eccentricity of load at balanced failure)

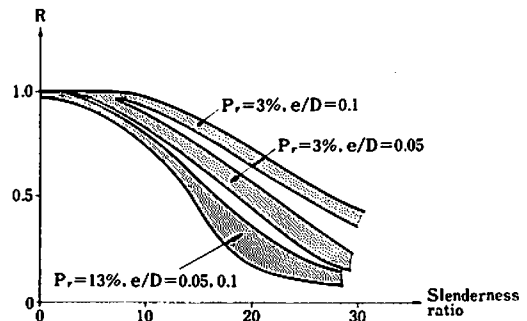


Fig. 8 Effect of spiral reinforcement on load carrying capacity of member (R:Ratio of increase in load carrying capacity by spiral reinforcement to that by steel pipe,  $P_s$ :Ratio of volume of spiral to the total volume, e:Eccentricity of load at the end of the member, D:Diameter of cross section)



## CONCLUSIONS

(1) It is clarified that the proposed analytical method can trace the effect of spiral reinforcement in a composite column subjected to bending moment in addition to axial load until the maximum loading capacity is reached. In order to evaluate the effect of spiral reinforcement, it is important to express the behaviour of mortar under the tri-axial stresses as a simple formula. In this analysis, regarding the behaviour of mortar confined with spiral reinforcement, volumetric strain and axial stress are assumed to be the sum of that without spiral reinforcement and that increased by the influence of spiral reinforcement.

(2) The effect of spiral reinforcement on the ultimate strength of cross section is similar to the effect of increasing the strength of mortar. Therefore, spiral reinforcement is quite effective to sustain the axial load, and it is similar to that of increasing the thickness of the steel pipe when the eccentricity of load is less than about 20 percent of the eccentricity at balanced failure. However, it is reduced as the eccentricity of load increases. For example, it becomes smaller than 50 percent of the effect of increasing the thickness of the steel pipe when the eccentricity is larger than the eccentricity at balanced failure.

(3) As the spiral reinforcement becomes effective only after the strain of mortar or the deflection of member is extremely large, the load carrying capacity of the member is not so effectively increased by using the spiral reinforcement as seen in the cross section. For example, the effectiveness of spiral reinforcement becomes to be less than that of increasing the thickness of the steel pipe when the slenderness ratio is larger than about 10, even when the effectiveness on the section is similar.

## ACKNOWLEDGMENTS

The authors would like to acknowledge financial support from Japan Railway Construction Public Corporation. Grateful acknowledgment is made to Prof. Dr. Yoshiro Higuchi who guided the support. Thanks are also made to Mr. Matsuji Enomoto, Technical Officer, University of Tokyo and the people of Nihon Consultant Co., Ltd. for their contributions to the experiments.

## REFERENCES

- 1) Sadahiko Adachi, Yoshiro Higuchi, Kei Tsuchiya and Michiyuki Sugiyama, "Strength of Composite Columns with Spiral Reinforcement," Railway Technical Research Report, No. 789, 1971, Dec. (In Japanese)
- 2) Japan Railway Construction Public Corporation and Nihon Consultant Co., Ltd., "Seiken 49-308 — Test Results on Composite Columns Reinforced with Spirals," 1975, Mar. (In Japanese)
- 3) Richard W. Furlong, "Design of Steel-Encased Concrete Beam-Columns," Journal of the Structural Division, Proceedings of the American Society of Civil Engineers, Vol. 94, No. ST 1, Jan., 1968, pp. 267-281.
- 4) Noel J. Gardner, "Use of Spiral Welded Steel Tubes in Pipe Columns," Journal of A.C.I., 1968, Nov., No. 65-70, pp. 937-942.